Biosensors and Bioelectronics 30 (2011) 188–196

Contents lists available at SciVerse ScienceDirect

Biosensors and Bioelectronics

journal homepage: www.elsevier.com/locate/bios

Development of DNA electrochemical biosensor based on immobilization of ssDNA on the surface of nickel oxide nanoparticles modified glassy carbon electrode

Abdollah Noorbakhsh[a,c], Abdollah Salimi[a,b,*]

[a] Department of Chemistry, University of Kurdistan, P.O. Box 416, Sanandaj, Iran
[b] Research Center for Nanotechnology, University of Kurdistan, P.O. Box 426, Sanandaj, Iran
[c] Department of Nanotechnology Engineering, Faculty of Advanced Science and Technology, University of Isfahan, 81746-73441 Isfahan, Iran

ARTICLE INFO

Article history:
Received 27 July 2011
Received in revised form 8 September 2011
Accepted 13 September 2011
Available online 1 October 2011

Keywords:
Nickel oxide nanoparticles
DNA hybridization
Electrochemical sensor
Taxon: 32630 tumor necrosis factor (TNF)

ABSTRACT

A sensitive electrochemical method for DNA hybridization based on immobilization of DNA probe and $[Ru(NH_3)_5Cl]PF_6$ complex onto nickel oxide nanomaterials ($NiOx_{np}$) modified glassy carbon electrode was developed. Due to strong affinity of $NiOx_{np}$ for phosphate groups, oligonucleotides probe with a terminal 5′-phosphate group was attached to the surface of the modified electrode. DNA immobilization and hybridization were characterized by electrochemical impedance spectroscopy (EIS) and differential pulse voltammetry using $K_3Fe(CN)_6/K_4Fe(CN)_6$ and $[Ru(NH_3)_5Cl]PF_6$ as probe and indicator, respectively. The Ru-complex current response indicates only the complementary sequence showing an obvious current signal in comparison to non-complementary and three or single point mismatched sequences. The fabricated biosensor possessed good selectivity and sensitivity for complementary probe, taxon: 32630 tumor necrosis factor (TNF). The linear dynamic range, sensitivity and detection limit of the proposed biosensor were 4×10^{-10} M to 1×10^{-8} M, 34.32 nA nM^{-1} and 6.8×10^{-11} M, respectively. Excellent reproducibility and stability, quite simple and inexpensive preparation are the other advantages of proposed biosensor.

1. Introduction

Rapid and simple determination of specific sequences DNA targets associated with either genetic or pathogenic diseases has become increasingly important not only in molecular diagnostics (Zhang et al., 2008; Escosura-Muniz et al., 2007; J.H. Chen et al., 2008; Zhang et al., 2006), but also in pharmaceutical and forensic applications (Mateo-Martí et al., 2007; Soper et al., 2006). Nucleic acid hybridization has become a fundamental technique in molecular biology for the detection and analysis of specific DNA sequences. Optical, piezoelectric or electrochemical instruments are often used in DNA biosensors as transducers (Watterson et al., 2002; Yang et al., 1997; Ligaj et al., 2006). A variety of techniques have been developed for the detection of DNA hybridization, including fluorescent (Dharmadi and Gonzales, 2004), radiochemical (Jilbert, 2000), piezoelectric (Wang et al., 2007), surface plasmon resonance spectroscopy (Yang et al., 2007), quartz crystal microbalance (Liu et al., 2004), electrophoretic (Landers, 2003), electrochemiluminescence (Miao and Bard, 2004), enzymatic (Castro et al., 2004), atomic force microscopy (Sun and Yokota, 2000) and electrochemical methods (Kang et al., 2007; Wang et al., 2001; Pan and Rothberg, 2005; Sun et al., 2008). Electrochemical detection assays have important advantages including, simplicity, reliability, sensitivity and selectivity. So a variety of approaches have been explored in electrochemical detection of DNA hybridization (Tang et al., 2006; Fan et al., 2005; Luo et al., 2006; Erdem, 2007; Luo et al., 2006). The key step for fabrication of DNA electrochemical biosensors is effective combination of ssDNA layers with electrochemical transducers. Effective immobilization of ssDNA probe onto the transducer surface through suitable method improve the performance of DNA based biosensors (Feng et al., 2008). Therefore, increasing the immobilization amount and controlling over the molecular orientation of oligonucleotides probe upgrade the detection limit of DNA biosensor (Fang et al., 2008). During the past decade, many efforts have been devoted to explore new supporting materials and immobilization methods for the fabrication of DNA biosensors. The combination of biological molecules and novel nanomaterials components is of great importance in developing new nanoscale devices for biological, medical and electronic

* Corresponding author at: Research Center for Nanotechnology, University of Kurdistan, P.O. Box 416, Sanandaj, Iran. Tel.: +98 871 6624001; fax: +98 871 6624008.
E-mail addresses: absalimi@yahoo.com, absalimi@uok.ac.ir (A. Salimi).

0956-5663/$ – see front matter © 2011 Elsevier B.V. All rights reserved.
doi:10.1016/j.bios.2011.09.010

applications (Willner, 2002). Electrodes modified with different nanomaterials such as carbon nanotubes (Qi et al., 2007) nanogold (Fang et al., 2008), silver nanoparticles/carbon nanotubes (Zhang et al., 2009b) and gold nanoparticles/carbon nanotubes/polyaniline nanofibers (Zhou et al., 2009) have been used for immobilization of DNA probes. Nanomaterials increase the surface area of electrode and enhance the amount of immobilized DNA probe. Metal oxide nanostructures such as nickel oxide, manganese oxide, zirconium oxide, titanium oxide, tungsten oxide, iridium oxide, iron oxide, zinc oxide and copper oxide are suitable matrixes and novel candidates for immobilization of enzymes and proteins due to their high electrical conductivity, wide electrochemical working window, high biocompatibility, large surface area, no toxicity, chemical and photochemical stability, electrochemical activity, ease of preparation and excellent substrate adhesion (Salimi et al., 2007). Nickel oxide nanoparticles can be used for immobilization of different biomolecules and electron transfer mediators entrapment (Salimi et al., 2008, 2007, 2006; Moghaddam et al., 2008; Mohammadi et al., 2009; Noorbakhsh and Salimi, 2009). Several methods including physical adsorption, entrapment in a gel or polymer film, covalent binding, cross-linking and electrochemical polymerization (Qi et al., 2007) have been used for immobilizing biomolecules and DNA probes onto electrode surfaces. In general, entrapment techniques are easy to perform, but the bonding of biomolcules is often weak. As a result biomolecules can leach out from the electrode which affects the significant signal loss and biosensor stability. Immobilization via amino groups of the guanine or one of the ends (5′ or 3′) of nucleic acids has also reported (Watterson et al., 2002; Sun et al., 1998; Zhao et al., 1999; Millan et al., 1994; Liu et al., 1996). The attachment of ss-DNA at one end increase the efficiency of the hybridization reaction, because proper packing density of nucleic acids chains, structural flexibility and orientation control in this method are assured (Ligaj et al., 2006; Pividori et al., 2000; Mikkelsen, 1996). Phosphonates and 5′-terminal phosphate group of ssDNA show strong attachment to a number of metal oxides including aluminum, titanium, zirconium and zinc oxides (Lin and Chen, 2005; Marafon et al., 2009; Xu et al., 2009). Nickel oxide nanoparticles have been attached to the biomolecules containing phosphate group such as 2′-deoxyguanosine 5′-monophosphate (Jezowska-Bojczuk et al., 2004) 2′-deoxyguanosine 5′-triphosphate (Kaczmarek et al., 2005) and Lathyrus Sativus (Panda et al., 2007). This thin oxide layer could therefore be exploited for DNA probe immobilization through phosphate-metal oxide attachment. To our best knowledge, NiOx nanoparticles have not been used for immobilization of DNA probe.

Many protocols have been proposed for electrochemical monitoring of DNA hybridization mainly based on the current signal generated by direct oxidation of guanine base (Erdem et al., 2004) or by double strand DNA intercalators, such as cationic metal complex (Li et al., 2008; Ligaj et al., 2006; Steichen et al., 2007), anticancer drug (Zhang et al., 2009a,b; Erdem and Ozsoz, 2001) organic dyes (Zuo et al., 2009; Zhou et al., 2009; Yau et al., 2003), redox label of the DNA probe (Qi et al., 2007) and enzymatic signal generation (Pan, 2007). Electrochemical detection of DNA hybridization using DNA intercalators has been received much attention due to its much more simplicity compared with the using of redox label and its higher sensitivity compared with that based on direct oxidation of guanine base. In the present study, the ssDNA probe sequences related to the taxon: 32630 tumor necrosis factor (TNF) (Buonaguro et al., 1992) was immobilized on the surface of GC electrode modified with $NiOx_{np}$ and $Ru[(NH_3)_5Cl]PF_6$ complex is used as an electroactive indicator. The sensor showed excellent and selective response toward complementary target at nanomolar or lower concentration range.

2. Experimental

2.1. Reagent

$Ni(NO_3)_2$, dimethyl sulfoxide (DMSO) and sodium dodecyl sulphate(SDS) were purchased from Merck. $Ru[(NH_3)_5Cl]PF_6$ was synthesized as reported (Takeuch et al., 1984). Bovine serum albumin (BSA) was purchased from Sigma. Three 21-mer synthetic oligonucleotides were purchased from Bioneer Company (China).

Their base sequences are as follows:

Immobilized probe ssDNA (S_1): 5′-PO_4-GGG GGG CCA AGG CCC AGC CCT CAC ACA-3′.
Target ssDNA (S_2, complementary to S1): 5′-TGT GTG AGG GCT GGG CCT TGG-3′.
Noncomplementray ssDNA (S_3): 5′-GGT TCC GGG TCG GGA GTG TGT-3′.
Three-base mismatch ssDNA (S_4): 5′-TGT CTG AGC GCT CGG CCT TGG-3′.
Single base mismatch ssDNA(S_5): 5′-TGT GTG AGC GCT GGG CCT TGG-3′.

All oligonucleotides were dissolved in 0.02 M PBS buffer (pH7.4) and kept frozen. Phosphate buffer solutions (PBS) (0.1 M) are prepared form H_3PO_4, KH_2PO_4 and K_2HPO_4. The pH of buffer solutions was adjusted with HCl and KOH solutions. Pure N_2 (99.999%) was passed through the solution to avoid possible oxidation during the experiments. All other chemicals were of analytical reagent grade and double distilled water (DDW) was used throughout.

2.2. Apparatus and instrumentations

Cyclic voltammetric (CV) and differential pulse voltammetric (DPV) measurements were performed with a computer controlled μ-Autolab modular electrochemical system (Eco Chemie Ultecht, The Netherlands), driven with GPES software (Eco Chemie). A three-electrode system was employed with Pt wire as auxiliary electrode, Ag/AgCl (saturated KCl) as reference electrode and glassy carbon (GC) electrode or modified GC electrode as the working electrode. Electrochemical impedance spectroscopy (EIS) was performed on an AUTOLAB modular electrochemical system (ECO Chemie, Ultrecht, The Netherlands) equipped with a PSTA 20 module and driven by GPES (ECO Chemie).

2.3. Electrodeposition of nickel oxide nanoparticles

Glassy carbon electrode (2 mm diameter) was carefully polished with alumina on polishing cloth. The electrode was placed in ethanol container and used bath ultrasonic cleaner in order to remove adsorbed particles. Nickel oxihydroxide film was electrodeposited on the surface of glassy carbon electrode from 1 mM nickel-chloride pH 4 phosphate buffer solution, using repetitive potential cycling (30 cycles at 100 mV s^{-1}) between 0.0 and −1.1 V. The potential was repetitively cycled (30 scans) from 0 to 1 V at a scan rate of 100 mV s^{-1} in fresh phosphate solution free of nickel ions for the electrodissolution and passivation of a nickel oxide layer at a GC electrode (Giovanelli et al., 2003). Modified electrode was eventually washed with double distilled water and stored at ambient temperature (25 °C) before being used in experiments.

2.4. Immobilization of ssDNA on nickel oxide nanoparticles modified GC electrode

The probe ss-DNA-modified electrode was obtained by pipetting 10 μL of probe ssDNA (S_1) onto the surface of $NiOx_{np}$ nanoparticles modified electrode and the casting solution was allowed to absorb

at room temperature for 60 min. Then, ssDNA-modified electrode was rinsed vigorously with 0.01 M PBS containing 0.1% sodium dodecyl sulphate (SDS) in order to wash out the non-immobilized probe DNA from the electrode surface before hybridization (Zhu et al., 2005). Finally, the modified electrode was immersed in BSA solution (1%, w/w in pH 7.4 PBS buffer) in order to blocking the active site of the electrode surface. The target ssDNA-modified electrodes thus obtained were denoted as $S_1/NiOx_{np}/GC$ in the text. The resulting DNA biosensor was stored in PBS at 4 °C when not in use.

2.5. Hybridization on target S_1-modified electrode

The hybridization reaction was performed by immersing $S_1/NiOx_{np}/GC$ electrode in 0.050 M PBS (pH 7.0) containing different concentrations of complementary target (S_2), noncomplementary (S_3), three bases mismatches (S_4) and one base mismatches (S_5) for 1 h at 37 °C. After hybridization, the obtained electrodes were washed with the PBS and water to remove non-specifically bound DNA. The electrodes thus obtained were denoted as $S_1–S_2/NiOx_{np}/GC$, $S_1–S_3/NiOx_{np}/GC$, $S_1–S_4/NiOx_{np}/GC$ and $S_1–S_5/NiOx_{np}/GC$, respectively. The approach to probe DNA immobilization and hybridization with target oligonucleotides is shown (Scheme 1 of Supplement).

2.6. Indicator binding

The Ru-complex was accumulated onto the ss-DNA/$NiOx_{np}/GC$ or ds-DNA/$NiOx_{np}/GC$ modified electrodes by immersing the electrodes into the stirred 0.05 mM $Ru[(NH_3)_5Cl]PF_6$ solution for 10 min at 30 °C. The obtained electrodes were then rinsed with PBS for 30 s and denoted as Ru-$S_1/NiOx_{np}/GC$ for ss-DNA and Ru-$S_1–S_2/NiOx_{np}/GC$, Ru-$S_1–S_3/NiOx_{np}/GC$, Ru-$S_1–S_4/NiOx_{np}/GC$, Ru-$S_1–S_5NiOx_{np}/GC$ for ds-DNA.

2.7. Electrochemical detection

The electrochemical characteristics of the modified electrode were characterized by EIS, CV and DPV techniques. EIS measurement was performed in 1.0 mM $K_3Fe(CN)_6/K_4Fe(CN)_6$ (1:1) mixture containing 0.1 M KCl with the frequencies ranging from 10^4 to 0.1 Hz. CV and DPV measurements were performed in 0.1 M PBS (pH 7.4). The DPV parameters were considered as follows: pulse amplitude 25 mV, pulse width 50 ms and scan rate 10 mV s^{-1}.

2.8. Regeneration of the modified electrode

The electrodes obtained after DNA hybridization were regenerated by rinsing the hybridized surfaces with hot (75 °C) double distilled water (DDW) for 3 min, followed by rapid cooling in ice bath. The reusability of the biosensor was tested by repetitive hybridization with target ss-DNA and regeneration (Li et al., 2007).

3. Results and discussion

3.1. Characterization of nickel oxide nanoparticles modified electrode

The formation of nickel oxide layer on the electrode surface was checked by recording the cyclic voltammogram of the modified electrode in alkaline solution (Fig. 1A of Supplement). After nickel dissolution and oxide formation in alkaline solution, the anodic peak at 0.48 V is observed due to the oxidation of the $Ni(OH)_2$ phase to NiO(OH). The corresponding cathodic peak at 0.41 V represents the reduction of NiO(OH) to $Ni(OH)_2$ (Giovanelli et al., 2003). For bare GC electrode no redox response was observed at potential range 0.0–0.7 V. The formation and growth of the nickel oxide nanoparticles on glassy carbon electrode was also investigated by taking scanning electron moicroscopy (SEM) image (Fig. 1 B of Supplement). As shown, nickel oxide particles have grown by electrodeposition on the amorphous glassy carbon surface. This image shows that that a uniform film of nickel oxide nanostructures with an average diameter ranging from 30 to 50 nm electrodeposited on the GC electrode.

3.2. Electrochemical behavior of $Ru[(NH_3)_5Cl]PF_6$

For investigation electrochemical properties of $[Ru(NH_3)_5Cl]PF_6$ complex cyclic voltammetry is used. Cyclic voltammograms of the GC electrode and GC-$NiOx_{np}$ modified electrode in DMSO solution containing 50 μM $Ru[(NH_3)_5Cl]PF_6$ complex at different scan rates are recorded (Fig. 1). As shown for GC electrode the cathodic and anodic peak potentials and peak potential separation (ΔE_p) are −0.506 V, −0.416 V and 90 mV (Fig. 1A), while at GC-$NiOx_{np}$ modified electrode these values are −0.385 V, −0.300 V and 80 mV (Fig. 1B), respectively. Furthermore, the peak currents are increased two times at GC/$NiOx_{np}$ in compared to bare GC electrode. This property indicates that the reaction is semi-reversible. For both GC and GC/$NiOx_{np}$ electrodes cathodic and anodic peak currents were increased with increasing square root of scan rate over the range of 100–500 mV s^{-1}. Therefore, the electrochemical redox reaction is a diffusion controlled process.

The cyclic voltammograms of GC electrode at different scan rates in phosphate buffer solution (pH 7) containing 50 μM $Ru[(NH_3)_5Cl]PF_6$ complex are recorded (Fig. 2 of Supplement). As can be seen in cathodic scan two separated peaks observed at −0.15 and −0.3 V, while at reverse scan only one peak observed at −0.1 V. With increasing the scan rate the peak current for second cathodic peak decreased, while the first anodic peak current increased, which indicate the chemical reaction followed with redox process. The peak current was proportional to the square root of scan rate over the range of 20–200 mV s^{-1}. Therefore, the electrochemical redox reaction is a diffusion controlled process. Cyclic voltammograms of GC/$NiOx_{np}$-$S_1–S_2$ modified electrode in buffer solution (pH 7) containing 50 μM $Ru[(NH_3)_5Cl]PF_6$ complex are recorded at different scan rates (Fig. 3 of Supplement). As shown the cathodic and anodic peak potentials are −0.05 V and 0.0 V, respectively. These results indicate the peak currents linearly increased with increasing the scan rate as expected for redox surface controlled process. These results indicate the Ru-complex immobilized onto $NiOx_{np}/S_1–S_2$ biocomposite.

3.3. Electrochemical study on the interaction between $[Ru(NH_3)_5Cl]PF_6$ and DNA

To explore the application of $[Ru(NH_3)_5Cl]PF_6$ in electrochemical DNA biosensors, electrochemical study on the interaction of $Ru[(NH_3)_5Cl]PF_6$ with DNA was performed. Cyclic voltammograms of 75 μM $Ru[(NH_3)_5Cl]PF_6$ in DMSO solution in the absence (voltammogram "a") and presence of DNA(voltammogram "b") are shown in Fig. 2A. As can be seen after interaction Ru-complex with DNA, both cathodic and anodic peak currents decreased and its formal potential shifted to the positive potential. These results indicate formation of a new association complex between DNA and Ru-complex. According to the previous research (Carter et al., 1989) intercalative binding of small molecules with DNA shifted formal potential ($E^{0\prime}$) to more positive value, while electrostatic binding displaced $E^{0\prime}$ to negative potential value. Although the electrostatic interaction between aptamer molecules and $[Ru(NH_3)_5Cl]^{2+}$ complex has been observed (Wang et al., 2009), in this study the ruthenium complex with only one positive charge was used, which causes the weak electrostatic interaction with DNA

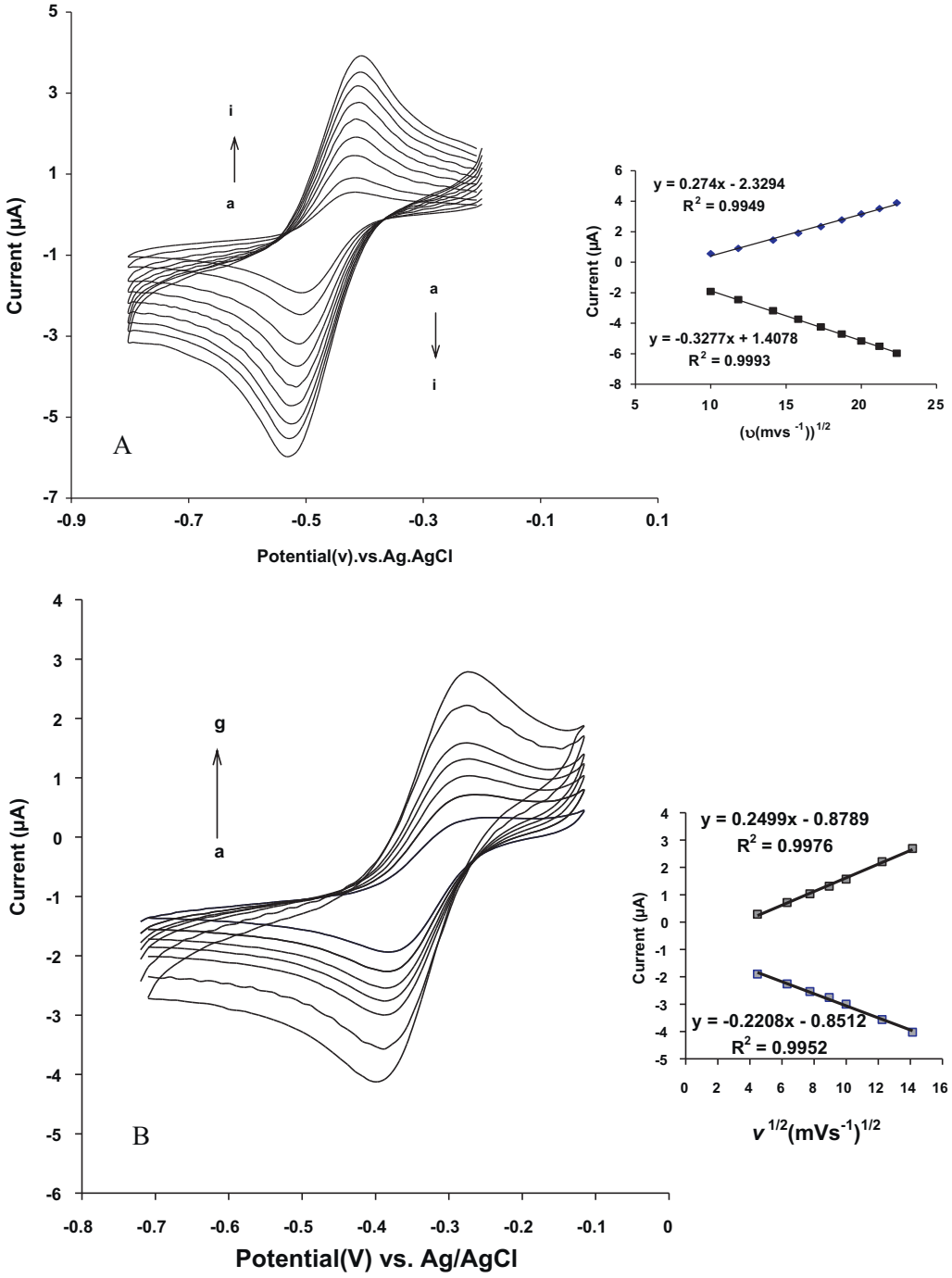

Fig. 1. (A) Cyclic voltammograms of glassy carbon electrode in DMSO solution containing 50 μM $Ru[(NH_3)_5Cl]PF_6$ complex at scan rates of (a) 100, (b) 140, (c) 200, (d) 250, (e) 300, (f) 350, (g) 400, (h) 450 and (i) 500 mV s^{-1}. (B) Cyclic voltammograms of GC-$NiOx_{np}$ modified electrode in DMSO solution containing 50 μM $Ru[(NH_3)_5Cl]PF_6$ complex at scan rates of (a) 20, (b) 40, (c) 60, (d) 80, (e) 100, (f) 150, and (g) 200 mV s^{-1}. Insets are plots of peak currents vs. the square root of scan rates.

molecules. Therefore, both intercalative and electrostatic interaction could be possible between $Ru[(NH_3)_5Cl]PF_6$ and DNA. The potential shift to positive values after interaction Ru-complex with DNA indicates intercalative attraction and stacking interactions of $Ru[(NH_3)_5Cl]PF_6$ between base pair of ds-DNA, which overcome the electrostatic attractions (Niu et al., 2006; J. Chen et al., 2008; Del Pozo et al., 2005; Li et al., 2008)

3.4. Electrochemical characteristics of the developed DNA biosensor

DPVs of $NiOx_{np}$/GC electrode, $S_1/NiOx_{np}$/GC electrode and $S_1–S_2/NiOx_{np}$/GC electrode after immersion for 10 min in 50 μM $Ru[(NH_3)_5Cl]PF_6$ and rinsing with washing solution, 0.1 M PBS (pH 7) are given in Fig. 2B. As shown on $NiOx_{np}$/GC electrode, no anodic

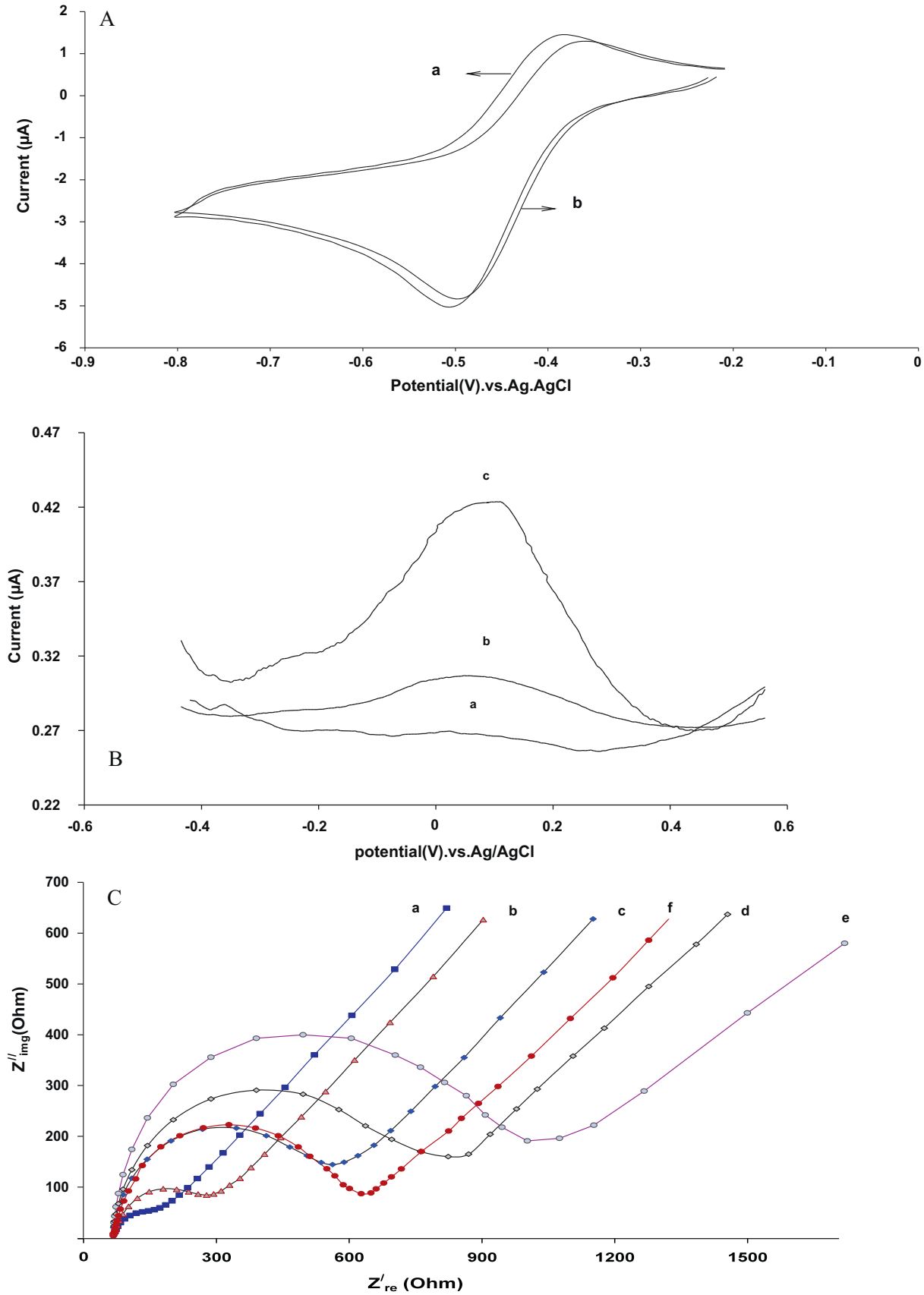

Fig. 2. (A) Cyclic voltammograms of glassy carbon electrode in DMSO solution containing (a) 50 μM $Ru[(NH_3)_5Cl]PF_6$ complex and (b) Mixture of 75 μM $Ru[(NH3)_5Cl]PF_6$ complex and 10 μM ds-DNA at the scan rate of 200 mV s^{-1}. (B) DPVs of (a) Ru-$NiOx_{np}$/GC, (b) Ru-S_1/$NiOx_{np}$/GC, (c) Ru-S_1–S_2/$NiOx_{np}$/GC in PBS phosphate buffer pH 7 at the scan rate of 10 mV s^{-1}. (C) Nyquist plots for GC electrode (a), $NiOx_{np}$/GC electrode (b), S_1/$NiOx_{np}$/GC electrode (c) S_1/$NiOx_{np}$/GC electrode after BSA immobilization (d), S_1–S_2/$NiOx_{np}$/GC (e) and S_1–S_2/$NiOx_{np}$/Ru-complex/GC (f) in 0.1 M KCl solution containing 1 mM $[Fe(CN)_6]^{3-/4-}$.

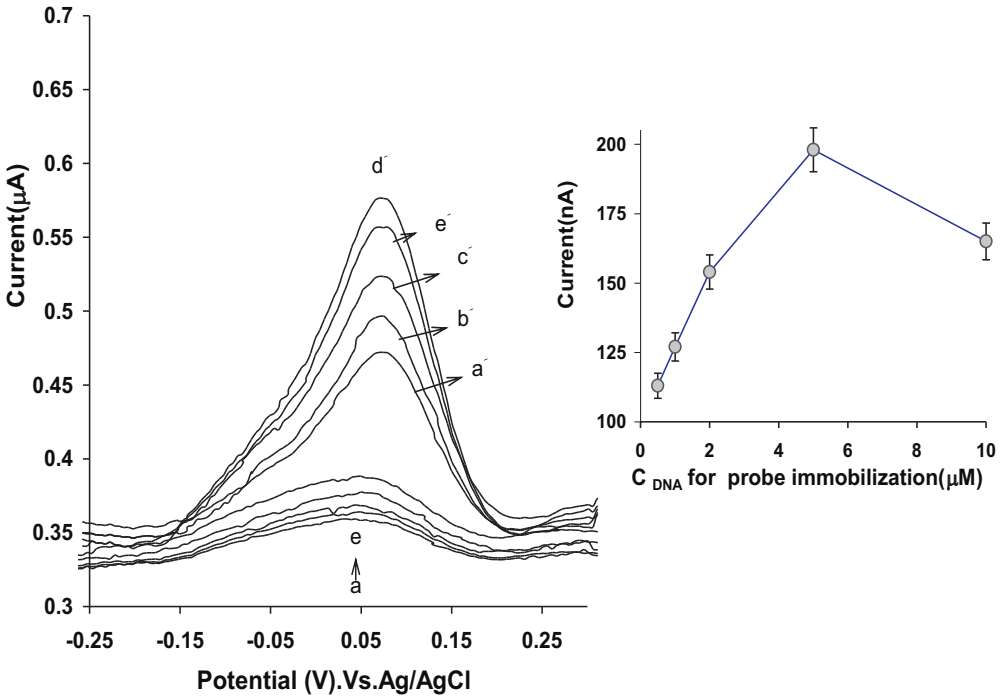

Fig. 3. DPVs of (a–e) S_1/$NiOx_{np}$/GC electrode after various S_1 probe concentrations used for probe immobilization (a) 0.5 μM, (b) 1 μM, (c) 2 μM, (d) 5 μM and (e) 10 μM. (a′–e′) S_1–S_2/$NiOx_{np}$/GC electrode, (a′) same as (a), (b′) same as (b), (c′) same as (c), (d′) same as (d) and (e′) same as (e) after hybridization with 10 nM complementary S_2 probe. Inset shows plot of peak current vs. S_1 probe concentration which used for probe immobilization.

response was observed for Ru-complex (curve a) due to less accumulation of $Ru[(NH_3)_5Cl]PF_6$ on the nickel oxide nanoparticles. However, for Ru-S_1/$NiOx_{np}$/GC electrode, a anodic response (curve b) was observed due to weak adsorption of $Ru[(NH_3)_5Cl]PF_6$ on the ss-DNA. As can be seen, a significant anodic peak corresponding to $Ru[(NH_3)_5Cl]PF_6$ oxidation appeared for Ru-S_1–S_2/$NiOx_{np}$/GC electrode (curve c). The phenomenon further proved the formation of ds-DNA (S_1–S_2) on the $NiOx_{np}$/GC electrode surface and the incorporation of $Ru[(NH_3)_5Cl]PF_6$ on S_1–S_2/$NiOx_{np}$/GC electrode surface.

Electrochemical impedance spectroscopy (EIS) analysis was performed to provide further evidence for interface assembly on electrode and to study the interface properties of the developed biosensor. Fig. 2C shows the Nyquist plots obtained for bare GC electrode (a), $NiOx_{np}$/GC electrode (b), S_1/$NiOx_{np}$/GC electrode (c), S_1/$NiOx_{np}$/GC electrode after interaction with BSA (d) and S_1/$NiOx_{np}$/GC electrode after interaction with BSA and 2 nM complementary S_2 probe (S_1–S_2/$NiOx_{np}$/GC electrode) (e). As shown, significant differences in the electron transfer resistance (R_{et}) were observed upon the stepwise formation of the modified electrodes. The bare GC electrode almost exhibits a straight line (plot a), which is a characteristic for a diffusion limited electrochemical process. For $NiOx_{np}$/GC electrode the value of R_{et} increases due to semiconductive properties of nickel oxide nanoparticle (plot b). Since the negative charge of ssDNA phosphate groups repulse the Fe $(CN)_6^{4-/3-}$ molecules and cause more electron transfer resistance, further increasing in electron transfer resistances (R_e) is observed when ssDNA was immobilized on the $NiOx_{np}$/GC electrode surface (plot c). After blocking the active site of the electrode with BSA the electron transfer resistance increases due to adsorption of BSA on the electrode surface (plot d). The higher electron transfer resistance was observed for the S_1–S_2/$NiOx_{np}$/GC electrode (plot e). A more negative charge of phosphate group on the electrode surface causes more repulsion of the $Fe(CN)_6^{4-/3-}$ molecules. After accumulation of Ru-complex, onto S_1–S_2/$NiOx_{np}$/GC electrode, the Rct is decreased (plot f), which indicate that Ru-complex as electron-shuttling mediator decreased electron transfer resistance. Based on the EIS results, we can conclude that S_1 DNA probe was successfully immobilized on $NiOx_{np}$/GC electrode and S_2 DNA was successfully hybridized with S_1 DNA probe.

3.5. Optimization of DNA hybridization conditions

In order to get desirable response for electrochemical detection of DNA hybridization, important experimental parameters including the concentration of ss-DNA probe (S_1) solution for immobilization of S_1 probe on the surface of $NiOx_{np}$/GC electrode and interaction time of $Ru[(NH_3)_5Cl]PF_6$ with DNA and hybridization time were optimized.

3.5.1. Optimization of immobilized probe concentration

During the performed experiments for developing DNA biosensor, it is found that surface concentration of immobilized DNA probe influences on the electrochemical signal of the biosensor. To get maximum signal response, surface concentration of S_1 DNA probe was optimized, using various concentration of S_1 DNA for immobilization process on the surface of $NiOx_{np}$/GC electrode. Fig. 3 illustrates the peak current of DNA biosensor after hybridization with 10 nM complementary target ss-DNA (S_2) vs. different concentration of S_1 probe. As shown, the peak currents rapidly increases with the S_1 probe concentration from 5.0×10^{-7} to 5.0×10^{-6} M, then reaches to the maximum value at 5.0×10^{-6} M. When S_1 concentration was higher than 5.0×10^{-6} M, the peak current decreases due to strict effect for hybridization events. Therefore, 5.0×10^{-6} M of S_1 was chosen as optimum value in order to obtain a high sensitivity in the subsequent experiment (Fig. 4).

3.5.2. Optimization of hybridization time

In order to optimize the hybridization time, the effect of the hybridization time on the peak uenc-base mismatch ss-DNA (S_4) and single-base mismatch ss-DNA(S_5). Fig. 5 shows the DPVs of S_1/$NiOx_{np}$/GC electrode after hybridization with 10 nM S_2, 10 nM S_3, 10 nM S_4 and 10 nM S_5 DNA sequences. As

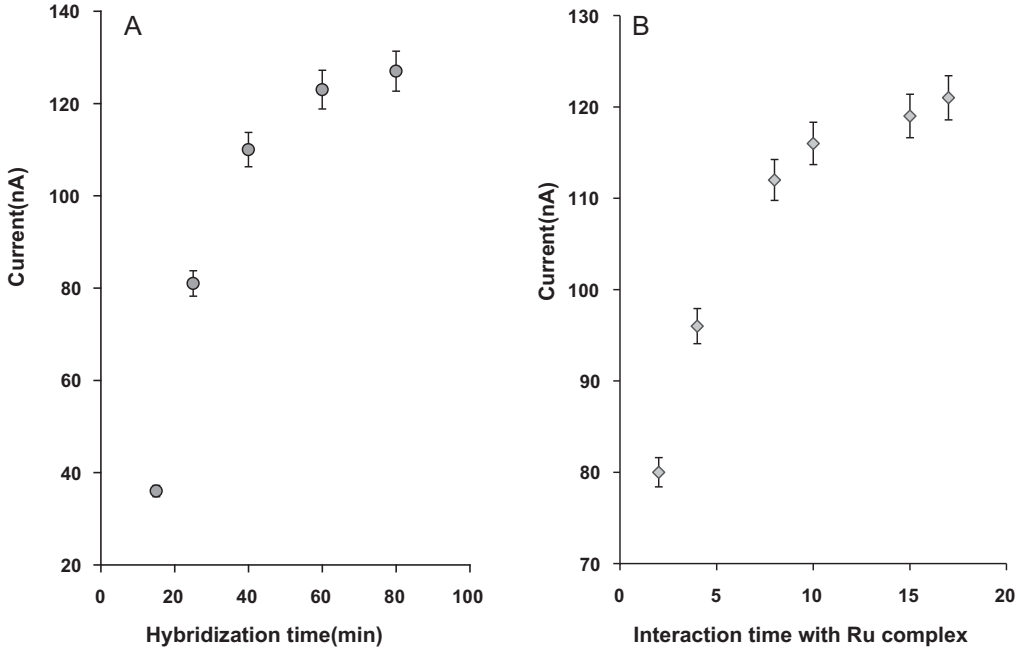

Fig. 4. (A) Plot of current vs. Hybridization time and (B) plot of current vs. Interaction time with Ru complex obtained for $S_1/NiOx_{np}$/GC electrode after hybridization with 5 nM complementary S_2 probe.

shown, after hybridization noncomplementary ss-DNA sequence with ss-DNA probe no change observed in compared to the response of Ru-$S_1/NiOx_{np}$/GC electrode. Furthermore, for Ru-S_1–$S_4/NiOx_{np}$/GC electrode a weak signal also can be observed. For single base mismatch S_1–$S_5/NiOx_{np}$/GC electrode the response (voltammogram e) is low in compared with complementary probe (S_2) (voltammogram b).The largest peak current is obtained for Ru-S_1–$S_2/NiOx_{np}$/GC electrode. These results indicate that almost no hybridization reaction takes place when the DNA biosensor detects three-base mismatched, one base mismatched and noncomplementary DNA sequences and this DNA biosensor detects only complementary ssDNA (S_2) selectively.

Fig. 6 shows the DPVs of $S_1/NiOx_{np}$/GC electrode after hybridization with various concentration of complementary S_2 probe in the range of 0.4 nM to 20 nM under optimized condition. As can be seen, with increasing concentration of S_2, the oxidation signal is also increased. The plot of peak current verses S_2 concentration is illustrated in inset Fig. 6. The linear regression equation for the concentration range from 0.4 nM to 10 nM was obtained as I (nA) = 20.8 C (nM) + 6.5 nA, R^2 = 0.9974, indicating that the regression line is fitted very well with the experimental data, and the regression equation can be applied in the unknown sample determination. For lower concentration range (Fig. 6B), the following equation between peak current and the S_2 concentration was found; I (nA) = 34.325 C (nM) − 0.12 nA, R^2 = 0.999. The detection

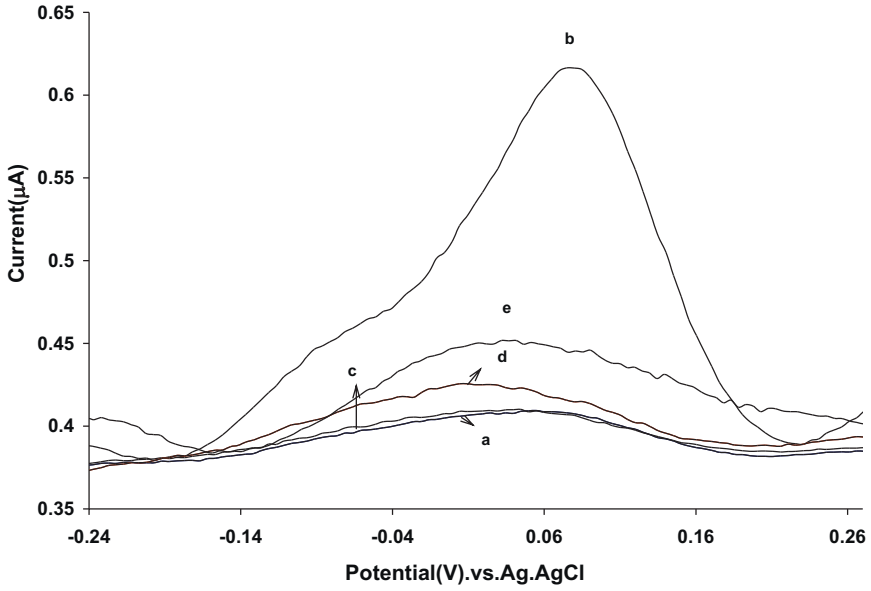

Fig. 5. DPVs of (a) $S_1/NiOx_{np}$ electrode, (b) S_1–$S_2/NiOx_{np}$ electrode, (c) S_1–$S_3/NiOx_{np}$ electrode, (d) S_1–$S_4/NiOx_{np}$ electrode and (e) S_1–$S_5/NiOx_{np}$ electrode in 0.1 M phosphate buffer pH7 at scan rate of 10 mV s^{-1}.

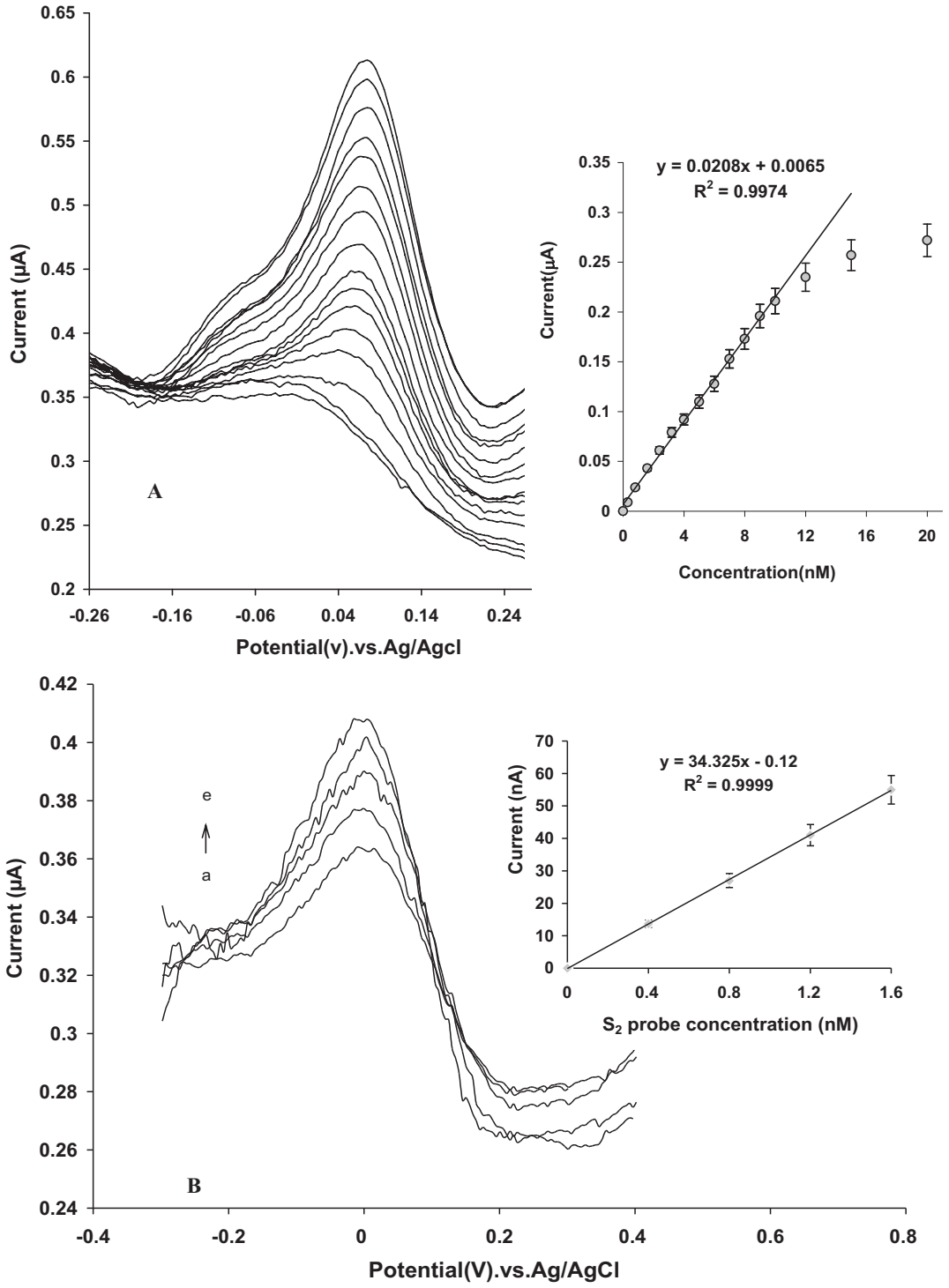

Fig. 6. DPVs of S_1–S_2/$NiOx_{np}$ electrode at different target DNA (S_2) concentration: inner to outer 0, 0.4, 0.8, 1.6, 2.4, 3.2, 4, 5, 6, 7, 8, 9, 10, 12, 15 and 20 nM, other condition as Fig. 5. Inset shows the plot of peak current vs. (S_2) concentration. (B) Enlarged voltammograms for lower concentrations of S_2, (a) 0.0, (b) 0.4, (c) 0.8, (d) 1.2 and (e) 1.6 nM.

limit was estimated as 68 pM when the signal to noise ratio is 3. The limit of quantification (LOQ) was 230 pM at signal to noise ratio of 10. The linear concentration range and detection limit of the proposed sensor are compared with various electrochemical DNA sensors.

3.6. Regeneration and reproducibility of DNA biosensor

The regeneration of DNA sensor was evaluated by measuring the intercalated $Ru[(NH_3)_5Cl]PF_6$ after DNA sensor hybridized with 3×10^{-9} M complementary oligonucleotides (S_2). After electrochemical measurement, the DNA sensor was regenerated according to the above process (Section 2.8). After four regeneration and hybridization, the electrode possessed 96% of its original current response. RSD of repeated peaks current was 5.5% ($n = 4$). The reproducibility of the DNA sensor was also investigated. Six DNA sensors were independently fabricated under the same experimental condition (S_1 probe concentration 5.0×10^{-6} M). The prepared sensors were used to detect 5×10^{-9} M of complementary oligonucleotides

(S_2). The RSD of six oxidation peak current was 4.5%. These results indicate that the DNA sensor shows a desirable repeatability and reproducibility.

4. Conclusion

Single stranded oligonucleotide DNA can be directly deposited onto $NiOx_{np}$ modified glassy carbon electrode using simple technique without complex surface modification or chemical cross linkers. $NiOx_{np}$ film could greatly enhance the loading of DNA probe and improved the sensitivity for the target DNA detection. The immobilization and hybridization of the DNA probe was characterized by CV, DPV and EIS techniques. High degree of sensitivity and selectivity were achieved by DPV experiments with $Ru[(NH_3)_5Cl]PF_6$ as a promising alternative intercalator for electrochemical detection of DNA hybridization. The proposed DNA sensor shows a good analytical performance for the specific sequences of DNA detection and it can discriminate completely complementary target sequence from noncomplementary, three and single base-mismatched DNA sequences. The developed DNA electrochemical biosensor possessed a high sensitivity and regeneration ability. The biosensor for detection of the target sequence, taxon: 32630 tumor necrosis factor (TNF) has relatively wide linear range (4×10^{-10} M to 1×10^{-8} M), low detection limit (6.8×10^{-11} M) with a high sensitivity (34.325 nA nM^{-1}) and good selectivity.

Acknowledgments

This work was financially supported by the Iranian Nanotechnology Initiative and the Research Office of the University of Kurdistan. The authors thank Dr. Saied Soltanian for taking SEM image.

Appendix A. Supplementary data

Supplementary data associated with this article can be found, in the online version, at doi:10.1016/j.bios.2011.09.010.

References

Buonaguro, L., Barillari, G., Chang, H.K., Bohan, C.A., Kao, V., Morgan, R., Gallo, P.C., Ensoli, B., 1992. J. Virol. 66, 7159–7167.
Carter, M.T., Rodriguez, M., Bard, A.J., 1989. J. Am. Chem. Soc. 111, 8901–8911.
Castro, A., Dalvit, D.A.R., Paz-matos, L., 2004. Anal. Chem. 76, 4169–4174.
Chen, J., Zhang, J., Zhuang, Q., Chen, J., Lin, X., 2008. Electrochim. Acta 53, 2716–3223.
Chen, J.H., Zhang, J., Zhuang, Q., Chen, J., Lin, X.H., 2008. Electrochim. Acta 53, 2716–2723.
Del Pozo, M.V., Alonso, C., Pariente, F., Lorenzo, E., 2005. Anal. Chem. 77, 2550–2557.
Dharmadi, Y., Gonzales, R., 2004. Biotechnol. Prog. 20, 1309–1324.
Erdem, A., 2007. Talanta 74, 318–325.
Erdem, A., Ozsoz, M., 2001. Anal. Chim. Acta 437, 107–114.
Erdem, A., Pividori, M.I., del Valle, M., Alegret, S., 2004. J. Electroanal. Chem. 567, 29–37.
Escosura-Muniz, A.D.L., González-García, M.B., Costa-García, A., 2007. Biosens. Bioelectron. 22, 1048–1054.
Fan, C.H., Plaxco, K.W., Heeger, A.J., 2005. Trends Biotechnol. 23, 186–192.
Fang, B., Jiao, S., Li, M., Qu, Y., Jiang, X., 2008. Biosens. Bioelectron. 23, 1175–1179.
Feng, L., Chen, W., Zhang, S., 2008. Biosens. Bioelectron. 24, 781–786.
Giovanelli, D., Lawrence, N.S., Wilkins, S.J., Jiang, L., Jones, T.G.L., Compton, R.G., 2003. Sens. Actuators B 88, 320–328.
Jezowska-Bojczuk, M., Kaczmarek, P., Bal, W., Kasprzak, K.S., 2004. J. Inorg. Biochem. 98, 1770–1777.
Jilbert, A.R., 2000. Methods Mol. Biol. 123, 177–193.
Kaczmarek, P., Jezowska-Bojczuk, M., Bal, W., Kasprzak, K.S., 2005. J. Inorg. Biochem. 99, 737–746.
Kang, J.W., Li, X.N., Wu, G.F., Wang, Z.H., Lu, X.Q., 2007. Anal. Biochem. 364, 165–170.
Landers, J.P., 2003. Anal. Chem. 75, 2919–2927.
Li, X.M., Ju, H.Q., Ding, C.F., Zhang, S.S., 2007. Anal. Chim. Acta 582, 158–163.
Li, F., Chen, W., Zhang, S., 2008. Biosens. Bioelectron. 24, 781–786.
Ligaj, M., Jasnowska, J., Grzegorz Musiał, W., Filipiak, M., 2006. Electrochim. Acta 51, 5193–5198.
Lin, K.C., Chen, S.M., 2005. J. Electroanal. Chem. 578, 213–222.
Liu, S., Ye, L., He, P., Fang, Y., 1996. Anal. Chim. Acta 335, 239–246.
Liu, T., Tang, J.A., Jiang, L., 2004. Biochem. Biophys. Res. Commun. 313, 3–7.
Luo, X.L., Morrin, A., Killard, A.J., Smyth, M.R., 2006. Electroanalysis 18, 319–326.
Marafon, E., Kubota, T., Gushikem, L.Y., 2009. J. Solid State Electrochem. 13, 377–438.
Mateo-Martí, E., Briones, C., Pradier, C.M., Martín-Gago, J.A., 2007. Biosens. Bioelectron. 22, 1926–1932.
Miao, W.J., Bard, A.J., 2004. Anal. Chem. 76, 5379–5386.
Mikkelsen, S.K., 1996. Electroanalysis 8, 15–19.
Millan, K.M., Saraullo, A., Mikkelsen, S.R., 1994. Anal. Chem. 66, 2943–2948.
Moghaddam, A.B., Ganjali, M.R., Dinarvand, R., Ahadi, S., Saboury, A.A., 2008. Biophys. Chem. 134, 25–33.
Mohammadi, A., Moghaddam, A.B., Kazemzad, M., Dinarvand, R., Badraghi, J., 2009. Mater. Sci. Eng. C 29, 1752–1758.
Niu, S.Y., Zhang, S.S., Wang, L., Li, X.M., 2006. J. Electroanal. Chem. 597, 111–118.
Noorbakhsh, A., Salimi, A., 2009. Electrochim. Acta 54, 6312–6321.
Pan, S.L., Rothberg, L., 2005. Langmuir 21, 1022–1027.
Pan, J., 2007. Biochem. Eng. J. 35, 183–190.
Panda, G.C., Das, S.K., Bandopadhyay, T.S., Guh, A.K., 2007. Colloids Surf. B 57, 135–142.
Pividori, M.I., Merkoci, A., Alegret, S., 2000. Biosens. Bioelectron. 15, 291–297.
Qi, H., Li, X., Chen, P., Zhang, C., 2007. Talanta 72, 1030–1035.
Salimi, A., Sharifi, E., Noorbakhash, A., Soltanian, S., 2007. Biosens. Bioelectron. 22, 3146–3153.
Salimi, A., Noorbakhash, A., Sharifi, E., Semnani, A., 2008. Biosens. Bioelectron. 24, 792–798.
Salimi, A., Sharifi, E., Noorbakhash, A., Soltanian, S., 2006. Electrochem. Commun. 8, 1499–1508.
Soper, S.A., Brown, K., Ellington, A., Frazier, B., Garcia-Manero, G., Gau, V., Gutman, S.I., Hayes, D.F., Korte, B., Landers, J.L., Larson, D., Ligler, F., Majumdar, A., Mascini, M., Nolte, D., Rosenzweig, Z., Wang, J., Wilson, D., 2006. Biosens. Bioelectron. 21, 1932–1942.
Steichen, M., Decrem, Y., Gosdfroid, E., Buess-Herman, C., 2007. Biosens. Bioelectron. 22, 2237–2243.
Sun, H.B., Yokota, H., 2000. Anal. Chem. 72, 3138–3141.
Sun, W., Zhong, J.H., Qin, P., Jiao, K., 2008. Anal. Biochem. 377, 115–119.
Sun, X., He, P., Liu, S., Ye, L., Fang, Y., 1998. Talanta 47, 487–495.
Takeuchi, K.J., Thompson, M.S., Pipes, D.W., Meyer, T.J., 1984. Inorg. Chem. 23, 1845–1852.
Tang, X.W., Bansaruntip, S., Nakayama, N., Yenilmez, E., Chang, Y.L., Wang, Q., 2006. Nano Lett. 6, 1632–1636.
Wang, J., Meng, W., Zheng, X., Liu, S., Li, G., 2009. Biosens. Bioelectron. 24, 1598–1602.
Wang, J., Polsky, R., Xu, D., 2001. Langmuir 17, 5739–5741.
Wang, Q., Yang, X.H., Wang, K.M., 2007. Sens. Actuators B, 27–232.
Watterson, J., Piunno, P.A.E., Krull, U.J., 2002. Anal. Chim. Acta 469, 115–127.
Willner, I., 2002. Science 98, 2407–2408.
Xu, X., Jindal, V., Shahedipour-Sandvik, F., Bergkvist, M., Cady, N.C., 2009. Appl. Surf. Sci. 255, 5905–5909.
Yang, M., McGovem, M.E., Thompson, M., 1997. Anal. Chim. Acta 346, 259–275.
Yang, X.H., Wang, Q., Wang, K.M., Tan, W.H., Li, H.M., 2007. Biosens. Bioelectron. 22, 1106–1110.
Yau, H.C.M., Chan, H.L., Yang, M., 2003. Biosens. Bioelectron. 18, 873–879.
Zhang, G.J., Chua, J.H., Chee, R.E., Agarwal, A., Wong, S.M., Buddharaju, K.D., Balasubramanian, N., 2008. Biosens. Bioelectron. 23, 1701–1707.
Zhang, J., Song, S.P., Zhang, L.Y., Wang, L.H., Wu, H.P., Pan, D., Fan, C.H., 2006. J. Am. Chem. Soc. 128, 8575–8580.
Zhang, Y., Ma, H., Zhang, K., Zhang, S., Wang, J., 2009a. Electrochim. Acta 54, 2385–2391.
Zhang, Y., Zhang, K., Ma, H., 2009b. Anal. Biochem. 387, 13–19.
Zhao, Y.D., Pang, D.W., Hu, S., Wang, Z.L., Cheng, J.K., Dai, H.P., 1999. Talanta 49, 751–756.
Zhou, N., Yang, T., Jiang, C., Du, M., Jiao, K., 2009. Talanta 77, 1021–1026.
Zhu, N.N., Chang, Z., He, P.G., Fang, Y.Z., 2005. Anal. Chim. Acta 545, 21–26.
Zuo, S.H., Zhang, L.F., Yuan, H.H., Lan, M.B., Lawrance, A., Wei, G.G., 2009. Bioelectrochemistry 74, 223–226.